Contribution from Bell Laboratories, Murray Hill, New Jersey 07974, and the Department of Chemistry, University of Wisconsin, Madison, Wisconsin 53706

Stereochemical Systematics of Metal Clusters. Structural Characterization of Tetrameric Triphenylphosphine Silver Chloride. An Analysis of Bonded vs. Nonbonded Interactions in the Cubane-like $(R_3Y)_4M_4X_4$ Species

BOON-KENG TEO*[1a] and JOSEPH C. CALABRESE[1b]

Received March 26, 1976 AIC60232G

A three-dimensional x-ray characterization of $[(C_6H_5)_3P]_4Ag_4Cl_4$, obtained by reaction of silver chloride with triphenylphosphine, revealed a markedly distorted "cubane-like" structure in solid state. This cluster crystallizes from $CHCl_3/Et_2O$ in the centrosymmetric orthorhombic space group *Pbcn* with $a = 17.925$ (4) Å, $b = 20.778$ (15) Å, $c = 18.299$ (3) Å, $V = 6815$ (5) Å^3, and $Z = 4$. Least-squares refinements yielded the final reliability indices of $R_1 = 4.00\%$ and $R_2 = 4.40\%$ for 2054 independent reflections. The molecule, which conforms to a crystallographic C_2 symmetry, can be described as two interpenetrating tetrahedra of four silver and four triply bridging chlorine atoms forming a highly distorted cube with each silver atom being further coordinated to a triphenylphosphine ligand. The silver···silver distances range from 3.408 (1) to 3.797 (1) Å (3.633 Å (average)); the chlorine···chlorine distances vary from 3.649 (5) to 4.031 (3) Å (3.837 Å (average)), and the silver–chlorine bond lengths range from 2.532 (3) to 2.760 (3) Å (2.653 Å (average)). A detailed analysis of the stereochemical behavior of this molecule as well as other known members of the $(R_3Y)_4M_4X_4$ (R = C_6H_5, C_2H_5; Y = P, As; M = Cu, Ag; X = Cl, Br, I) family led to the unequivocal conclusion that their stereochemistries are to a significant extent dictated by intramolecular van der Waals repulsions.

Introduction

Recently there has been considerable interest in the stereochemistry and bonding of cubane-like metal cluster compounds of general formula $L_{4n}M_4X_4$.[2-41] The basic structure can be described as two interpenetrating tetrahedra of four metal (M) and four triply bridging ligands (X) situated on alternate corners of a distorted cube with each metal atom being further coordinated to one, two, or three terminal ligands (L).

Through extensive structural studies of closely related cubane-like metal clusters with strong metal–metal interactions such as $[(\eta\text{-}C_5H_5)_4Fe_4(CO)_4]^n$ (n = 0, 1+)[2,3] $[(\eta\text{-}C_5H_5)_4Fe_4S_4]^n$ (n = 0, 1+, 2+),[4-6] $(\eta\text{-}C_5H_5)_4Co_4P_4$,[7] $[(\eta\text{-}C_5H_5)_4Co_4S_4]^n$ (n = 0, 1+),[8] $(NO)_4Fe_4S_4$,[9] and $(NO)_4Co_4(NC(CH_3)_3)_4$[10] Dahl and co-workers have demonstrated that the systematic variations of the molecular geometry from the idealized T_d symmetry can be correlated with the alteration of valence electrons within these metal cluster systems. A unified molecular orbital theory[11] based upon the first-order Jahn–Teller effect as well as the symmetry properties and relative energetics of the orbitals was subsequently formulated to rationalize the existing and to predict the yet unknown molecular distortions of this type of compound.

However, this bonding model, which assumes that electronic effects predominate over steric ones, is incapable of rationalizing the statistically significant and generally *nonsystematic* deviation of the cubane core from the idealized T_d geometry frequently observed for cubane-like metal clusters containing no metal···metal bond.[15-32,35,37-41] It is also unable to account for the drastic stereochemical differences observed in a number of tetrameric copper complexes recently investigated by Churchill et al.[30-34] and others.[35,36] Although electronic considerations of these latter complexes indicate a completely nonbonding tetracopper core which in the absence of steric overcrowding would be expected to conform to cubic T_d geometry, it was found instead that these $L_4Cu_4X_4$ complexes possess in the crystalline state either a markedly distorted cubane-like structure, as exemplified by $(Ph_3P)_4Cu_4Cl_4$, $(Et_3P)_4Cu_4X_4$ (X = Cl, Br, I), and $(Et_3As)_4Cu_4I_4$, or a chair-like structure as illustrated by $(Ph_3P)_4Cu_4X_4$ (X = Br, I).

As part of a continuing effort to elucidate the intriguing stereochemical characteristics of transition metal cluster systems, we have focused our attention on a series of tetrameric triphenylphosphine silver halide clusters[38-40] with the hope of assessing the relative importance of bonded vs. nonbonded interactions (i.e., electronic vs. steric effects) in dictating the molecular structure of $(R_3Y)_4M_4X_4$-type complexes[28-41] (R = Ph, Et; Y = P, As; M = Cu, Ag; X = Cl, Br, I). This paper reports the preparation and structure of $(Ph_3P)_4Ag_4Cl_4$ which adopts a markedly distorted cubane-like configuration. A detailed analysis of the structural features of these clusters led to the unequivocal conclusion that their stereochemistries are to a significant extent dictated by intramolecular *nonbonded* van der Waals interactions which are a function of the size of the metal, the bridging, and the terminal ligands.

Experimental Data

$(Ph_3P)_4Ag_4Cl_4$ was prepared by reacting AgCl in saturated aqueous KCl solution with a stoichiometric amount of triphenylphosphine in ether under constant stirring at room temperature. The white precipitate (initially formed at the solution interface) in the ether phase was filtered and washed thoroughly with saturated KCl solution, water, ethanol, ether, vacuum-dried, and recrystallized from $CHCl_3/Et_2O$. Elemental analysis (Galbraith Laboratories, Knoxville, Tenn.) suggested the stoichiometry $(C_6H_5)_3PAgCl$. Anal. Calcd: C, 53.30; H, 3.73; P, 7.64; Cl, 8.74. Found: C, 54.58; H, 3.85; P 7.44; Cl, 8.43. Slow crystallization of $(Ph_3P)_4Ag_4Cl_4$ from $CHCl_3$/ether (vapor diffusion) afforded colorless rectangular crystals suitable for x-ray structural study. Details on crystal data, collection and reduction of the diffraction data, and solution and refinement of the structure are given in Table I.

The final positional and thermal parameters, with errors estimated from the full variance–covariance matrix, are listed in Tables II and III, respectively.

Results and Discussion

Description of the Structure. The crystal structure of $(Ph_3P)_4Ag_4Cl_4$ is composed of discrete molecules separated by van der Waals distances. It is both isomorphous and isostructural with the copper analogue $(Ph_3P)_4Cu_4Cl_4$.[32] The molecule conforms to the crystallographic C_2-2 site symmetry in the orthorhombic space group *Pbcn* (No. 60; D_{2h}^{14}).[42] The pertinent intramolecular distances and bond angles[46] are tabulated in Tables IV and V, respectively.

As shown[50] in Figures 1 and 2, the molecule adopts a cubane-like configuration with two interpenetrating tetrahedra of silver and chlorine atoms forming a markedly distorted cube, each silver atom being further coordinated to a triphenylphosphine ligand PPh_3.

The most striking structural feature of the molecular structure is that both the nonbonding and bonding distances of the M_4X_4 core deviate greatly from the idealized cubic T_d

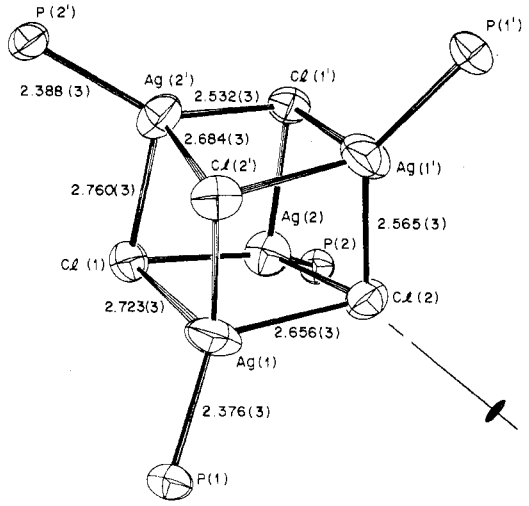

Figure 1. Highly distorted $P_4Ag_4Cl_4$ core of the cubane-like $(Ph_3P)_4Ag_4Cl_4$ molecule (ORTEP diagram, 50% probability ellipsoids) with crystallographic C_2-2 site symmetry.

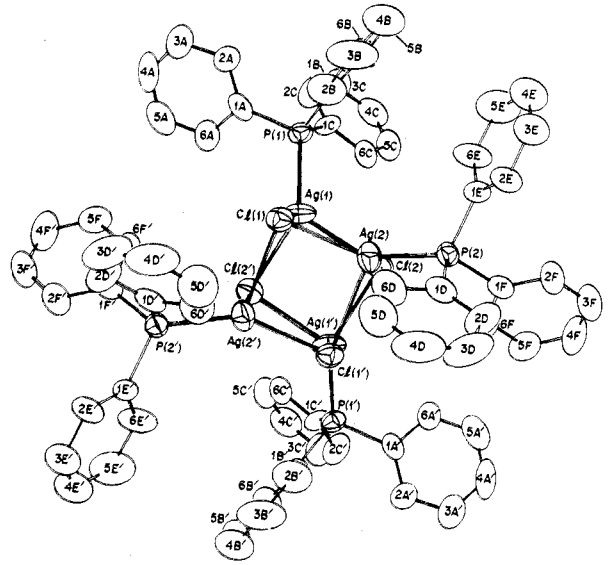

Figure 2. Stereochemistry of the $(Ph_3P)_4Ag_4Cl_4$ molecule.

geometry expected from bonding considerations. The unusual degree of the *nonsystematic* distortions manifest themselves in the following intracluster parameters: (1) the Ag···Ag distances range from 3.408 (1) to 3.797 (1) Å (3.633 Å (average)); (2) the Cl···Cl distances vary from 3.649 (5) to 4.031 (3) Å (3.837 Å (average)); (3) the Ag–Cl distances range from 2.532 (3) to 2.760 (3) Å (2.653 Å (average)). These intracubane core parameters possess the following characteristics. First, the Ag···Ag distances are best considered as *nonbonding* as judged from the fact that their arithmetic mean of 3.633 Å is 0.734 Å longer than the silver–silver distance of 2.899 Å observed in silver metal.[51] These distances are also comparable to that of 3.708 (3) Å observed in $[S(C_2H_4PPh_2)_2]_2Ag_2Cl_2$[52] which contains no silver–silver bond. Second, the nonbonding Cl···Cl distances are all greater than or close to the sum of van der Waals radii of chlorine (3.60 Å).[53] For each *nonplanar* Ag_2Cl_2 moiety a *short* Cl···Cl contact is accompanied in general by a *long* Ag···Ag distance and vice versa.[30,55] Third, all of the Ag–Cl bond lengths are substantially longer than the sum of covalent radii (viz., 2.33 Å).[54] The average value of 2.653 Å is, however, comparable to the corresponding value of 2.650 Å reported for $[S(C_2H_4PPh_2)_2]_2Ag_2Cl_2$.

Table I

(a) Crystal Data

Molecular Formula	$[(C_6H_5)_3PAgCl]_4$
Crystal shape, color	Rectangular block, colorless
Crystal dimensions, mm	0.43 × 0.18 × 0.10
Crystal face indices, distance from centroid, mm	±(1̄10, 0.08), ±(11̄0, 0.05), ±(001, 0.22)
Cell parameters (errors), Å	$a = 17.925$ (4), $b = 20.778$ (15), $c = 18.299$ (3)
Cell vol, Å^3	6815 (5)
Z	4
d_{calcd}, g/cm^3	1.581
d_{obsd}, g/cm^3	1.58
Laue symmetry	Orthorhombic
Space group	$Pbcn$ [D_{2h}^{14}; No. 60][42]
Systematic absences	$0kl, k = 2n + 1$; $h0l, l = 2n + 1$; $hk0, h + k = 2n + 1$
Equivalent positions	$\pm(x, y, z)$; $\pm(1/2 - x, 1/2 - y, 1/2 + z)$; $\pm(1/2 + x, 1/2 - y, z)$; $\pm(x, y, 1/2 - z)$

(b) Collection and Reduction of the X-ray Diffraction Data

Diffractometer	Syntex $P\bar{1}$
Radiation (graphite monochromated[43])	Mo Kα
Range of transmission	0.78–0.86[44]
μ, cm^{-1}	13.90
Mounting axis	c
Takeoff angle, deg	4
Scan speed (T_R),[45] deg/min	2–24
Scan range, deg	~2
Background:scan time ratio (B_R)[45]	0.67
Scan method	θ–2θ
No./freq of std reflections	2/50
Intensity variation of std reflections	±2%
2θ limits, deg	2–40
Cutoff of obsd data	2$\sigma(I)$[45]
Unique data[45]	3276
p[45]	0.055

(c) Solution and Refinement

Technique of solution	Heavy atom (Patterson)
Method of refinement	Full-matrix least squares[46,47]
Isotropic convergence[48]	$R_1 = 9.13\%$, $R_2 = 11.58\%$
Anisotropic convergence	$R_1 = 4.00\%$, $R_2 = 4.40\%$
Max shifts (Δ/σ)	0.07 (x, y, z), 0.15 (B's)
Error of fit	1.02
Data/parameter	2054/379
Anomalous dispersion cor[49]	
$\Delta f'$ (real)	−0.9 (Ag), 0.1 (P), 0.1 (Cl)
$\Delta f''$ (imag)	1.4 (Ag), 0.2 (P), 0.2 (Cl)
Max residual intensity of final diff map, e/Å^3	0.4

Further definitive evidence concerning the large deformation of the Ag_4Cl_4 core is given by the Ag–Cl–Ag angles ranging from 79.32 (7) to 92.67 (8)° (86.48° (average)) and the Cl–Ag–Cl angles varying from 87.23 (8) to 101.20 (8)° (92.72° (average)). Other salient structural features which have further implications include (1) average Ag–P bond lengths of 2.382 (3) Å (with a range of only 0.012 Å) being close to the sum of covalent radii of 2.44 Å[54] and (2) highly irregular P–Ag–Cl angles ranging from 109.9 (1) to 138.9 (1)° (122.35° (average)).

These unusual molecular deformations point to steric overcrowding among the ligands. Indeed, a detailed examination of intra- and intermolecular nonbonding separations revealed a wide spectrum of close van der Waals contacts, of the types (Ph)H···H(Ph) and (Ph)H···Cl listed in Table VI. It is apparent that the shortest ones are either close to or somewhat shorter than the sum of van der Waals radii—viz., H···H, 2.40 Å; H···Cl, 3.00 Å.[53] This strongly suggests that the stereochemistry of $(Ph_3P)_4Ag_4Cl_4$ is significantly perturbed by *weak* van der Waals interactions which have generally been ignored

Table II. Final Positional Parameters ($\times 10^4$) for $(Ph_3P)_4Ag_4Cl_4$ with Esd's

Atom	*x*	*y*	*z*
Ag(1)	943.3 (5)	534.9 (4)	2075.3 (5)
Ag(2)	608.6 (5)	1733.2 (4)	3304.1 (4)
Cl(1)	903.1 (14)	1840.8 (12)	1956.5 (13)
Cl(2)	392.2 (14)	459.3 (12)	3420.0 (14)
P(1)	2145.8 (15)	113.6 (13)	1812.8 (14)
P(2)	926.4 (16)	2291.2 (13)	4401.6 (14)
C(1A)	2349 (5)	86 (4)	850 (5)
C(2A)	3017 (6)	285 (5)	536 (5)
C(3A)	3126 (7)	226 (6)	−210 (6)
C(4A)	2571 (9)	−29 (6)	−633 (6)
C(5A)	1919 (8)	−217 (6)	−340 (7)
C(6A)	1800 (6)	−148 (5)	405 (5)
C(1B)	2911 (5)	579 (5)	2207 (5)
C(2B)	2873 (7)	1231 (5)	2175 (7)
C(3B)	3438 (7)	1623 (6)	2471 (9)
C(4B)	4022 (8)	1323 (7)	2800 (7)
C(5B)	4075 (7)	670 (7)	2852 (6)
C(6B)	3530 (6)	289 (5)	2533 (6)
C(1C)	2327 (5)	−701 (5)	2119 (5)
C(2C)	2784 (7)	−1123 (5)	1736 (6)
C(3C)	2966 (7)	−1716 (6)	2030 (7)
C(4C)	2673 (7)	−1917 (6)	2679 (7)
C(5C)	2205 (7)	−1511 (6)	3058 (6)
C(6C)	2009 (6)	−900 (5)	2777 (5)
C(1D)	483 (5)	3080 (5)	4427 (6)
C(2D)	236 (7)	3380 (5)	5046 (6)
C(3D)	−139 (8)	3981 (7)	4964 (8)
C(4D)	−206 (7)	4264 (6)	4313 (10)
C(5D)	50 (8)	3966 (7)	3695 (8)
C(6D)	390 (7)	3376 (5)	3738 (6)
C(1E)	1900 (5)	2434 (5)	4620 (5)
C(2E)	2161 (6)	2981 (6)	4971 (6)
C(3E)	2912 (7)	3014 (6)	5161 (6)
C(4E)	3390 (7)	2513 (7)	5039 (7)
C(5E)	3138 (7)	1978 (6)	4665 (8)
C(6E)	2378 (6)	1939 (6)	4446 (7)
C(1F)	582 (6)	1890 (5)	5225 (5)
C(2F)	886 (7)	1993 (6)	5905 (5)
C(3F)	605 (7)	1666 (6)	6508 (6)
C(4F)	43 (8)	1236 (6)	6421 (6)
C(5F)	−272 (6)	1134 (5)	5758 (6)
C(6F)	15 (6)	1450 (5)	5130 (5)
H(2A)[a]	3422	477	848
H(3A)	3601	371	−442
H(4A)	2659	−79	−1167
H(5A)	1518	−400	−662
H(6A)	1309	−270	614
H(2B)	2438	1441	1933
H(3B)	3396	2101	2449
H(4B)	4438	1592	2985
H(5B)	4496	465	3124
H(6B)	3573	−189	2532
H(2C)	2986	−997	1252
H(3C)	3317	−1998	1759
H(4C)	2791	−2352	2875
H(5C)	1998	−1642	3541
H(6C)	1653	−619	3043
H(2D)	314	3200	5548
H(3D)	−370	4190	5389
H(4D)	−439	4702	4258
H(5D)	−8	4176	3210
H(6D)	576	3160	3291
H(2E)	1826	3341	5089
H(3E)	3107	3416	5387
H(4E)	3910	2529	5212
H(5E)	3485	1617	4536
H(6E)	2197	1557	4173
H(2F)	1299	2309	5968
H(3F)	819	1742	6999
H(4F)	−140	980	6853
H(5F)	−715	845	5701
H(6F)	−189	1353	4639

[a] For all hydrogens $B = 7.0$ Å^2.

in the consideration of effects influencing the stereochemistry of metal cluster systems.

The two crystallographically independent triphenylphosphine ligands are normal with bond lengths and angles comparable to those observed in the copper homologue.[32] In particular, the six independent phosphorus–carbon bond distances range from 1.799 (9) to 1.828 (10) Å (averaging 1.817 Å) whereas the 36 independent carbon–carbon bond lengths range from 1.334 (18) to 1.426 (16) Å (averaging 1.381 Å). The six Ag–P–C angles, ranging from 110.7 (3) to 119.6 (3)°, are all greater than the ideal tetrahedral angle whereas the six C–P–C angles, ranging from 102.5 (4) to 105.5 (4)°, are all somewhat smaller than the ideal tetrahedral angle.[32] An interesting pattern is also observed for the 12 P–C–C angles (cf. Table V); viz., those oriented toward the pseudo-threefold axis of the triphenylphosphine are all greater than the ideal trigonal angle (122.5 (8)–124.9 (9)°) whereas those oriented in the opposite direction are all smaller than the ideal trigonal angle (114.9 (8)–118.3 (8)°). We believe that this signifies the weak intratriphenylphosphine phenyl···phenyl repulsions among the "inner" hydrogens—H(2A), H(6B), H(2C) in $Ph_3P(1)$ and H(2D), H(2E), H(2F) in $Ph_3P(2)$ (cf. Table VIA).

Stereochemical Systematics of $L_4M_4X_4$ Clusters. A detailed analysis of the interplay of electronic and steric effects is of prime importance in the basic understanding of the stereochemical systematics of metal cluster compounds. Table VII presents a comparison of pertinent molecular parameters for a number of cubane-like $(R_3Y)_4M_4X_4$ complexes where R = C_6H_5, C_2H_5; Y = P, As; M = Cu, Ag; and X = Cl, Br, I. The following general characteristics readily emerge: (1) the X···X distances are all greater than or close to normal van der Waals contacts (viz., Cl···Cl, 3.60 Å; Br···Br, 3.90 Å; I···I, 4.30 Å) suggesting that these halogen···halogen interactions are strongly repulsive thereby imposing a lower limit on the size of the *nonbonding* X_4 tetrahedron;[30] (2) the M···M distances, though considered as *nonbonding* (vide infra), exhibit a wide range of variation, indicating that the metal···metal interactions are relatively "soft";[30] (3) the M–X bond lengths are all significantly greater than normal covalent values (viz., Cu–Cl, 1.16 Å; Cu–Br, 2.31 Å; Cu–I, 2.50 Å; Ag–Cl, 1.33 Å; Ag–Br, 2.48 Å; Ag–I, 2.67 Å)[54] suggesting that the metal–halogen bonds are relatively weak; (4) for bulkyl R groups (such as phenyl) a significant molecular distortion from the optimal T_d geometry inevitably occurs as a result of intramolecular steric repulsions.

(I) "Bonded" Interactions. Qualitatively, for a cubane-like $(Ph_3P)_4Ag_4X_4$ cluster of presumed T_d geometry the five 4d orbitals per silver atom transform to give 20 symmetrized tetrametal orbitals of $a_1 + 2\,e + 2\,t_1 + 3\,t_2$ representations which, from overlap considerations, can be categorized as six bonding ($a_1 + e + t_2$), six antibonding ($t_1 + t_2$), and eight "essentially nonbonding" ($e + t_1 + t_2$) combinations. Similarly, the silver 5s and 5p orbitals transform as $a_1 + t_2$ and $a_1 + e + t_1 + 2\,t_2$, respectively, while the relevant phosphine σ orbitals and the four valence orbitals per halogen combine as $a_1 + t_2$ and $2\,a_1 + e + t_1 + 3\,t_2$, respectively. The symmetrized ligand orbitals are then presumed to interact with corresponding metal symmetry combinations of the same representation and appropriate overlap. From energetic considerations the 80 valence electrons available for bonding within the $P_4Ag_4X_4$ core can be allocated (via the Aufbau principle in increasing orbital energy) to $(a_1 + t_2)^8$ (halogen lone pairs), $(a_1 + t_2)^8$ (Ag–P bonding), $(a_1 + e + t_1 + 2\,t_2)^{24}$ (Ag–X bonding), $(a_1 + e + t_2)^{12}$ (Ag–Ag bonding), $(t_1 + t_2)^{12}$ (Ag–Ag antibonding), and $(e + t_1 + t_2)^{16}$ (essentially Ag–Ag nonbonding, partially Ag–X antibonding). This electronic configuration gives rise to two very important features: (1) complete occupation of both bonding ($a_1 + e + t_2$) and an-

Table III. Final Anisotropic Thermal Parameters ($\times 10^4$; with Esd's) for $(Ph_3P)_4Ag_4Cl_4$[a]

Atom	β_{11}	β_{22}	β_{33}	β_{12}	β_{13}	β_{23}
Ag(1)	25.4 (3)	27.6 (2)	53.2 (4)	5.7 (3)	8.3 (3)	−2.6 (3)
Ag(2)	40.7 (3)	29.4 (2)	29.1 (3)	−3.7 (3)	−7.1 (3)	−5.1 (3)
Cl(1)	27.3 (9)	20.8 (7)	30.6 (9)	−3.4 (8)	2.1 (8)	2.0 (7)
Cl(2)	30.8 (11)	20.9 (7)	32.3 (9)	0.8 (8)	−3.3 (8)	3.6 (7)
P(1)	22.2 (10)	20.6 (8)	28.7 (10)	4.7 (8)	5.0 (8)	0.3 (8)
P(2)	26.2 (10)	20.7 (8)	22.2 (9)	−2.5 (8)	−3.1 (9)	−0.3 (7)
C(1A)	26 (4)	17 (3)	28 (3)	7 (3)	−7 (3)	−2 (3)
C(2A)	30 (4)	33 (3)	28 (4)	1 (3)	2 (3)	3 (3)
C(3A)	51 (5)	36 (4)	34 (4)	7 (4)	6 (4)	4 (3)
C(4A)	81 (7)	36 (4)	24 (4)	11 (5)	−9 (4)	0 (3)
C(5A)	46 (5)	41 (4)	53 (5)	2 (4)	−17 (4)	−1 (4)
C(6A)	43 (5)	37 (4)	26 (4)	8 (4)	−2 (4)	−1 (3)
C(1B)	24 (4)	25 (3)	32 (4)	9 (3)	8 (3)	−3 (3)
C(2B)	41 (5)	23 (3)	70 (6)	−6 (4)	−2 (5)	−6 (4)
C(3B)	40 (6)	27 (4)	97 (7)	2 (4)	10 (5)	−13 (5)
C(4B)	43 (5)	48 (4)	67 (6)	−10 (5)	−2 (5)	−18 (4)
C(5B)	49 (5)	52 (5)	43 (5)	−3 (5)	−14 (4)	5 (4)
C(6B)	34 (5)	33 (4)	42 (4)	−2 (4)	−6 (4)	−1 (4)
C(1C)	26 (4)	24 (3)	29 (3)	3 (3)	6 (3)	−2 (3)
C(2C)	51 (5)	28 (3)	38 (4)	17 (4)	6 (4)	1 (3)
C(3C)	62 (6)	29 (4)	48 (5)	16 (4)	4 (5)	−1 (4)
C(4C)	46 (6)	26 (3)	62 (5)	2 (4)	−9 (4)	10 (4)
C(5C)	57 (6)	34 (4)	34 (4)	−4 (4)	−10 (4)	11 (3)
C(6C)	37 (5)	32 (3)	27 (4)	1 (4)	−3 (3)	−5 (3)
C(1D)	24 (4)	20 (3)	43 (4)	−6 (3)	−7 (3)	−4 (3)
C(2D)	55 (5)	22 (3)	47 (5)	−4 (4)	15 (4)	−8 (3)
C(3D)	54 (5)	29 (4)	78 (6)	−5 (4)	34 (5)	−5 (4)
C(4D)	39 (5)	26 (4)	113 (8)	6 (4)	11 (6)	7 (5)
C(5D)	68 (7)	40 (5)	58 (6)	16 (4)	−8 (5)	7 (4)
C(6D)	49 (5)	24 (3)	49 (5)	17 (4)	−12 (4)	0 (3)
C(1E)	20 (4)	23 (3)	29 (4)	−6 (3)	1 (3)	−2 (3)
C(2E)	26 (4)	34 (4)	44 (4)	−9 (3)	−4 (4)	−6 (3)
C(3E)	33 (5)	36 (4)	53 (5)	−9 (4)	−6 (4)	−9 (4)
C(4E)	41 (5)	41 (4)	60 (5)	−3 (4)	−6 (5)	9 (4)
C(5E)	40 (5)	33 (4)	88 (7)	12 (4)	3 (5)	−3 (4)
C(6E)	22 (4)	36 (4)	62 (5)	2 (4)	−1 (4)	−4 (4)
C(1F)	24 (4)	19 (3)	37 (4)	−1 (3)	−2 (3)	−2 (3)
C(2F)	48 (5)	50 (4)	24 (4)	−20 (4)	−8 (4)	10 (3)
C(3F)	62 (6)	38 (4)	31 (4)	−17 (4)	−10 (4)	2 (3)
C(4F)	68 (7)	39 (4)	23 (4)	−3 (4)	4 (4)	6 (3)
C(5F)	44 (5)	31 (4)	42 (5)	−18 (4)	10 (4)	2 (3)
C(6F)	42 (5)	24 (3)	28 (4)	0 (3)	−5 (4)	−2 (3)

[a] Of the form $\exp[-(h^2\beta_{11} + k^2\beta_{22} + l^2\beta_{33} + 2hk\beta_{12} + 2hl\beta_{13} + 2kl\beta_{23})]$.

tibonding ($t_1 + t_2$) tetrametal symmetry orbitals is consistent with the observed nonbonding Ag···Ag distances; (2) full occupation of the *partially* antibonding Ag–X ($e + t_1 + t_2$) orbitals which in weakening the Ag–X bonds is in accord with their highly variable, long distances.

This qualitative bonding model is also applicable to all complexes of the type $(R_3Y)_4M_4X_4$ listed in Table VII. It should be emphasized, however, that the band separation and the categorization of three types of metal orbitals are somewhat artificial. In fact, bands of similar energy can overlap and molecular orbitals of same symmetry representation can mix. Nevertheless, these simplified bonding models conceptually provide a reasonable qualitative basis for the stereochemical as well as physical properties of these cluster systems.

(II) "Nonbonded" Interactions. Realizing the composite effects of weak metal–ligand bonding and repulsive metal···metal and halogen···halogen interactions which render possible the severe distortions from T_d geometry or cleavage of the metal–halogen bonds for bulkyl terminal ligands, the observed structural variations of the known members of the series $(R_3Y)_4M_4X_4$ can be rationalized based on *nonbonded interactions* alone. In fact, some of the arguments presented in this section have been put forth independently by Churchill et al.[30-34]

For the following discussion, it is of interest to calculate the average distance of the terminal pnicogen atom (Y) from the centroid of the cubane core based on the average M···M distance. The results are listed in the last row of Table VII.

(a) Variation of R. For a given Y, M, and X, the effect of the R groups is twofold. First, the molecular symmetry is highly dictated by the size of the R groups, viz., the bulkier the R groups, the more likely is the distortion of the molecule from the idealized T_d symmetry due to the intramolecular nonbonded repulsions or intermolecular crystal packing forces. This is evident by comparing (1) $(Ph_3P)_4Cu_4Cl_4$ (**5**) with $(Et_3P)_4Cu_4Cl_4$ (**6**) [**5** has a crystallographically imposed C_2 symmetry with Cu···Cu, Cl···Cl, and Cu···Cl distances varying over the ranges of 0.31, 0.33, and 0.15 Å, respectively, whereas **6** has a crystallographically imposed T_d symmetry with no apparent distortion] and (2) $(Ph_3P)_4Ag_4I_4$ (**3**) with $(Et_3P)_4Ag_4I_4$ (**4**) [**3**, with no nontrivial symmetry property, has a highly distorted cubane structure as exemplified by the widely varying Ag···Ag, I···I, and Ag–I distances of ranges 0.65, 0.40, and 0.20 Å, respectively, whereas **4**, with a crystallographically imposed D_{2d} symmetry, has a much smaller distortion as indicated by the corresponding ranges of 0.03, 0.05, and 0.00 Å]. The variations in M–X–M, X–M–X, and Y–M–X angles follow similar trends (cf. Table VII). This is compatible with the estimated size of each phenyl ring being much larger than that of each ethyl group.[56]

Second, the bulkier phenyl groups apparently require a larger distance of the terminal ligands from the centroid of the cubane core: e.g., Y···O for $(Ph_3P)_4Cu_4Cl_4$ is 0.08 Å larger than the corresponding distance for $(Et_3P)_4Cu_4Cl_4$ (4.22 vs. 4.14 Å) whereas Y···O for $(Ph_3P)_4Ag_4I_4$ is 0.19 Å larger than the corresponding value for $(Et_3P)_4Ag_4I_4$ (4.59 vs. 4.40 Å).

Table IV. Interatomic Distances (A) with Esd's for $(Ph_3P)_4Ag_4Cl_4$

	A. Ag···Ag Distances		
Ag(1)···Ag(1)′	3.7217 (17)	Ag(1)···Ag(2)′	3.7973 (13)
Ag(1)···Ag(2)	3.4081 (12)	Ag(2)···Ag(2)′	3.6634 (16)
	B. Cl···Cl Distances		
Cl(1)···Cl(1)′	3.800 (5)	Cl(1)···Cl(2)′	3.756 (3)
Cl(1)···Cl(2)	4.031 (3)	Cl(2)···Cl(2)′	3.649 (5)
	C. Ag–Cl Bond Lengths		
Ag(1)–Cl(1)	2.7232 (26)	Ag(2)–Cl(1)	2.5316 (25)
Ag(1)–Cl(2)	2.6562 (26)	Ag(2)–Cl(1)′	2.7604 (27)
Ag(1)–Cl(2)′	2.5646 (27)	Ag(2)–Cl(2)	2.6836 (26)
	D. Ag–P Bond Lengths		
Ag(1)–P(1)	2.3755 (27)	Ag(2)–P(2)	2.3878 (26)
	E. P–C Bond Lengths		
P(1)–C(1A)	1.799 (9)	P(2)–C(1D)	1.823 (10)
P(1)–C(1B)	1.827 (10)	P(2)–C(1E)	1.815 (10)
P(1)–C(1C)	1.812 (10)	P(2)–C(1F)	1.828 (10)
	F. C–C Bond Lengths		
C(1A)–C(2A)	1.390 (13)	C(1D)–C(2D)	1.367 (13)
C(2A)–C(3A)	1.384 (13)	C(2D)–C(3D)	1.426 (16)
C(3A)–C(4A)	1.367 (16)	C(3D)–C(4D)	1.334 (18)
C(4A)–C(5A)	1.344 (17)	C(4D)–C(5D)	1.367 (18)
C(5A)–C(6A)	1.388 (14)	C(5D)–C(6D)	1.372 (15)
C(1A)–C(6A)	1.367 (13)	C(1D)–C(6D)	1.412 (14)
C(1B)–C(2B)	1.359 (14)	C(1E)–C(2E)	1.387 (13)
C(2B)–C(3B)	1.407 (16)	C(2E)–C(3E)	1.392 (13)
C(3B)–C(4B)	1.359 (17)	C(3E)–C(4E)	1.367 (16)
C(4B)–C(5B)	1.363 (17)	C(4E)–C(5E)	1.380 (17)
C(5B)–C(6B)	1.386 (15)	C(5E)–C(6E)	1.421 (16)
C(1B)–C(6B)	1.397 (13)	C(1E)–C(6E)	1.376 (13)
C(1C)–C(2C)	1.391 (13)	C(1F)–C(2F)	1.376 (13)
C(2C)–C(3C)	1.384 (15)	C(2F)–C(3F)	1.390 (14)
C(3C)–C(4C)	1.365 (15)	C(3F)–C(4F)	1.354 (15)
C(4C)–C(5C)	1.376 (15)	C(4F)–C(5F)	1.355 (14)
C(5C)–C(6C)	1.414 (15)	C(5F)–C(6F)	1.420 (13)
C(1C)–C(6C)	1.395 (12)	C(1F)–C(6F)	1.379 (13)

Table V. Bond Angles (deg) with Esd's for $(Ph_3P)_4Ag_4Cl_4$

	A. Ag–Cl–Ag Angles		
Ag(1)–Cl(1)–Ag(2)	80.78 (7)	Ag(1)–Cl(2)–Ag(1)′	90.92 (8)
Ag(1)–Cl(1)–Ag(2)′	87.65 (8)	Ag(1)–Cl(2)–Ag(2)	79.32 (7)
Ag(2)–Cl(1)–Ag(2)′	87.51 (8)	Ag(1)′–Cl(2)–Ag(2)	92.67 (8)
	B. Cl–Ag–Cl Angles		
Cl(1)–Ag(1)–Cl(2)	97.07 (8)	Cl(1)–Ag(2)–Cl(1)′	91.67 (8)
Cl(1)–Ag(1)–Cl(2)′	90.46 (8)	Cl(1)–Ag(2)–Cl(2)	101.20 (8)
Cl(2)–Ag(1)–Cl(2)′	88.67 (8)	Cl(1)′–Ag(2)–Cl(2)	87.23 (8)
	C. P–Ag–Cl Angles		
Cl(1)–Ag(1)–P(1)	112.03 (9)	Cl(1)–Ag(2)–P(2)	136.60 (9)
Cl(2)′–Ag(1)–P(1)	138.85 (9)	Cl(1)′–Ag(2)–P(2)	109.88 (9)
Cl(2)–Ag(1)–P(1)	120.20 (9)	Cl(2)–Ag(2)–P(2)	116.55 (9)
	D. P–Ag···Ag Angles		
P(1)–Ag(1)···Ag(1)′	155.36 (7)	P(2)–Ag(2)···Ag(1)	150.18 (8)
P(1)–Ag(1)···Ag(2)	124.22 (8)	P(2)–Ag(2)···Ag(1)′	130.31 (7)
P(1)–Ag(1)···Ag(2)′	150.38 (7)	P(2)–Ag(2)···Ag(2)′	144.85 (7)
	E. Ag–P–C Angles		
Ag(1)–P(1)–C(1A)	113.2 (3)	Ag(2)–P(2)–C(1D)	110.7 (3)
Ag(1)–P(1)–C(1B)	114.0 (3)	Ag(2)–P(2)–C(1E)	119.6 (3)
Ag(1)–P(1)–C(1C)	116.4 (3)	Ag(2)–P(2)–C(1F)	113.0 (3)
	F. C–P–C Angles		
C(1A)–P(1)–C(1B)	104.6 (4)	C(1D)–P(2)–C(1E)	105.5 (4)
C(1A)–P(1)–C(1C)	103.7 (4)	C(1D)–P(2)–C(1F)	104.0 (5)
C(1B)–P(1)–C(1C)	103.7 (5)	C(1E)–P(2)–C(1F)	102.5 (4)
	G. P–C–C Angles		
P(1)–C(1A)–C(2A)	124.7 (7)	P(2)–C(1D)–C(2D)	124.9 (9)
P(1)–C(1A)–C(6A)	116.7 (8)	P(2)–C(1D)–C(6D)	114.9 (8)
P(1)–C(1B)–C(2B)	118.3 (8)	P(2)–C(1E)–C(2E)	124.1 (8)
P(1)–C(1B)–C(6B)	122.5 (8)	P(2)–C(1E)–C(6E)	115.2 (8)
P(1)–C(1C)–C(2C)	122.6 (7)	P(2)–C(1F)–C(2F)	122.8 (8)
P(1)–C(1C)–C(6C)	118.1 (7)	P(2)–C(1F)–C(6F)	116.6 (7)
	H. C–C–C Angles		
C(2A)–C(1A)–C(6A)	118.6 (9)	C(2D)–C(1D)–C(6D)	120.2 (10)
C(1A)–C(2A)–C(3A)	120.2 (10)	C(1D)–C(2D)–C(3D)	117.7 (11)
C(2A)–C(3A)–C(4A)	119.3 (11)	C(2D)–C(3D)–C(4D)	121.5 (12)
C(3A)–C(4A)–C(5A)	121.3 (11)	C(3D)–C(4D)–C(5D)	120.6 (13)
C(4A)–C(5A)–C(6A)	119.7 (11)	C(4D)–C(5D)–C(6D)	120.4 (13)
C(1A)–C(6A)–C(5A)	120.8 (11)	C(1D)–C(6D)–C(5D)	119.5 (11)
C(2B)–C(1B)–C(6B)	119.3 (10)	C(2E)–C(1E)–C(6E)	120.6 (10)
C(1B)–C(2B)–C(3B)	121.6 (12)	C(1E)–C(2E)–C(3E)	118.9 (11)
C(2B)–C(3B)–C(4B)	117.4 (12)	C(2E)–C(3E)–C(4E)	121.8 (11)
C(3B)–C(4B)–C(5B)	122.8 (12)	C(3E)–C(4E)–C(5E)	119.3 (12)
C(4B)–C(5B)–C(6B)	119.3 (12)	C(4E)–C(5E)–C(6E)	119.9 (12)
C(1B)–C(6B)–C(5B)	119.6 (11)	C(1E)–C(6E)–C(5E)	119.3 (11)
C(2C)–C(1C)–C(6C)	119.3 (9)	C(2F)–C(1F)–C(6F)	120.5 (9)
C(1C)–C(2C)–C(3C)	120.3 (10)	C(1F)–C(2F)–C(3F)	119.9 (10)
C(2C)–C(3C)–C(4C)	121.3 (11)	C(2F)–C(3F)–C(4F)	120.0 (10)
C(3C)–C(4C)–C(5C)	119.0 (11)	C(3F)–C(4F)–C(5F)	121.2 (10)
C(4C)–C(5C)–C(6C)	121.3 (10)	C(4F)–C(5F)–C(6F)	120.0 (11)
C(1C)–C(6C)–C(5C)	118.6 (10)	C(1F)–C(6F)–C(5F)	118.2 (9)

The generally irregular distortions (i.e., nonsystematic scattering of the intracluster bond lengths and angles) strongly suggest that they are caused by intramolecular steric hindrance (presumably superimposed with anisotropic crystal packing forces) operating over the inherently flat potential surface in the absence of electronic or vibronic (Jahn–Teller) effects.

In order to facilitate the following discussions, idealized T_d geometry with averaged parameters will be utilized.

(b) Variation of X. Two homologous cubane-like series, $(Ph_3P)_4Ag_4X_4$ and $(Et_3P)_4Cu_4X_4$, have recently been structurally characterized, thus providing a detailed comparison of their stereochemistries within each series. The $(Ph_3P)_4Cu_4X_4$ series is also known; however, the conversion from a cubane-like structure for X = Cl[32] to a chair-like structure for X = Br[33] or I[34] precludes this type of comparison.

An examination of Table VII revealed three general trends. First, as the size of the triply bridging halogen atom increases along the sequence Cl < Br < I, (1) the average X···X distance increases, each corresponding to (or greater than) a normal van der Waals separation,[53] (2) the average M–X bond length increases as expected from the change in covalent radius of the halogen,[54] (3) the average M···M distance decreases (the disruption of this trend at $(Ph_3P)_4Ag_4Br_4$[39] is believed to be caused by the crystallographic C_3-3 constraint), and (4) the average M–Y distance increases slightly but significantly. The average intracluster angles respond correspondingly to these variations (cf. Table VII): the M–X–M angles decrease, the X–M–X angles increase, and the Y–M–X angles decrease as the size of the bridging halogens increases (vide infra). These changes are not unexpected in light of the fact that as the halogen atoms are replaced by their heavier congeners, the intramolecular nonbonding repulsions of types X···X, M···M, R···X, and R···R are enhanced significantly. As a result, the halogen atoms move outward (to relieve X···X repulsions) which, in order to maintain reasonable metal–halogen bond lengths, causes the metal atoms to move inward toward the centroid of the cubane-like core; the M–Y bonds are concomitantly lengthened slightly to help relieve the intensified repulsive R···X and R···R van der Waals interactions.

Second, as the bridging halogen atoms are replaced by their bulkier congeners, the terminal ligands are only slightly drawn in toward the centroid of the cubane-like core as evidenced by the small decrease in Y···O distances (again with the exception of $(Ph_3P)_4Ag_4Br_4$). This small change in Y···O distance is apparently due to the composite effect of the shrinkage of the metal tetrahedron counteracted by the lengthening of the M–Y bonds.

Finally, there is a general decrease in molecular symmetry (i.e., a larger degree of molecular distortion) as the size of the triply bridging atoms increases for cubane-like $(R_3Y)_4M_4X_4$ clusters with bulky terminal ligands (R_3Y). This is evidenced by a much more severe distortion in $(Ph_3P)_4Ag_4I_4$ of C_1

Table VI. Shortest van der Waals Contacts for $(Ph_3P)_4Ag_4Cl_4$

A. Intramolecular Cl···H(Ph) (<3.40 Å) and (Ph)H···H(Ph′) (<2.85 Å) Contacts			
Cl(1)···H(2B)	2.87	H(2D)···H(2F)	2.67
Cl(1)···H(6F)′ [a]	3.34	H(2D)···H(2E)	2.85
Cl(2)···H(6F)	3.08	H(5D)···H(5D)′	2.59
Cl(2)···H(6C)	3.26	H(2E)···H(2F)	2.84
B. Intermolecular Cl···H(Ph) (<3.40 Å) and (Ph)H···H(Ph′) (<2.85 Å) Contacts			
Cl(1)···H(3C)^{i} [a]	2.81	H(4B)···H(4B)^{vi}	2.69
Cl(1)···H(4C)^{i}	3.34	H(5B)···H(3D)^{vii}	2.83
Cl(2)···H(5A)^{ii}	2.63	H(5B)···H(5D)^{viii}	2.84
Cl(2)···H(4F)^{iii}	3.06	H(6C)···H(4F)^{iii}	2.82
Cl(2)···H(5F)^{iii}	3.20	H(3D)···H(5E)^{ix}	2.65
H(2A)···H(4D)^{iv}	2.61	H(3D)···H(4D)^{x}	2.79
H(4A)···H(6C)^{v}	2.73	H(4E)···H(6F)^{vii}	2.84
H(5A)···H(6E)^{v}	2.71	H(4F)···H(4F)^{xi}	2.42
H(3B)···H(4C)^{i}	2.54		

[a] The superscripts refer to the following symmetry transformations: (prime) $-x, y, {}^1/_2 - z$; (i) ${}^1/_2 - x, {}^1/_2 + y, z$; (ii) $x, -y, {}^1/_2 + z$; (iii) $-x, -y, 1 - z$; (iv) ${}^1/_2 + x, -{}^1/_2 + y, {}^1/_2 - z$; (v) $x, -y, -{}^1/_2 + z$; (vi) $1 - x, y, {}^1/_2 - z$; (vii) ${}^1/_2 + x, {}^1/_2 - y, 1 - z$; (viii) ${}^1/_2 - x, -{}^1/_2 + y, z$; (ix) $-{}^1/_2 + x, {}^1/_2 - y, 1 - z$; (x) $-x, 1 - y, 1 - z$; (xi) $-x, y, {}^3/_2 - z$.

symmetry in comparison to $(Ph_3P)_4Ag_4Cl_4$ of C_2 symmetry. We believe this is caused by intensified van der Waals nonbonded interactions of the type (Ph)H···H(Ph) and (Ph)H···X for larger X.[40] However, this effect can be disrupted by crystallographically imposed constraints as exemplified by the C_3 geometry of $(Ph_3P)_4Ag_4Br_4$.

(c) Variation of M. Replacement of the copper atoms by the much larger silver atoms causes a significant expansion of the cubane-like core. For example, comparison of $(Ph_3P)_4Ag_4Cl_4$ (**1**) with $(Ph_3P)_4Cu_4Cl_4$ (**5**) indicates an increase of 0.261, 0.327, 0.209, and 0.189 Å in average Cl···Cl, M···M, M–Cl, and M–P distances, respectively, in going from **5** to **1**. As a consequence of these comparable increases in interatomic distances, the bond angles in **1** and **5** are very similar (cf. Table VII). Similarly, there are increases of 0.373, 0.381, 0.235, and 0.184 Å for average I···I, M···M, M–I, and M–P, respectively, in going from $(Et_3P)_4Cu_4I_4$ (**8**) to $(Et_3P)_4Ag_4I_4$ (**4**). The expansion of the cubane-like core in this latter pair is even more homogeneous than in the previous one, resulting in virtually identical M–X–M, X–M–X, and Y–M–X angles.

This expansion of the cubane-like core also manifests itself in average Y···O distances shown in Table VII. The average Y···O distance increases by 0.39 and 0.36 Å for the pairs $(Ph_3P)_4M_4Cl_4$ and $(Et_3P)_4M_4I_4$ (M = Cu → Ag), respectively. The relief in intramolecular nonbonding repulsive interactions presumably renders possible the existence of cubane-like structures for all members of the series $(Ph_3P)_4Ag_4X_4$ but changes the solid-state structure in favor of the chair form on going from $(Ph_3P)_4Cu_4Cl_4$ to $(Ph_3P)_4Cu_4X_4$ (X = Br, I) (vide supra).

(d) Variation of Y. There is only one comparison that can be made between two systems with a different terminal ligand atom (Y) but otherwise similar structure: $(Et_3P)_4Cu_4I_4$ (**8**) vs. $(Et_3As)_4Cu_4I_4$ (**9**). Granting that intramolecular nonbonding interactions dictate to a large extent the stereochemistry of these systems, replacement of the phosphorus atom in **8** by the much larger arsenic atoms in **9** (Cu–As in **9** is 0.11 Å longer than Cu–P in **8**) apparently relieves steric repulsions of the types Et(H)···(H)Et and Et(H)···I, thereby allowing the slight expansion of the iodine tetrahedron with a concomitant shrinkage of the copper tetrahedron (cf. Table VII). As a consequence, the Cu–I and Y···O distances in **8** and **9** are very similar while Cu–I–Cu (I–Cu–I) decreases (increases) from 66.10 (4)° (109.38 (4)°) in **8** to 62.63 (5)° (111.45 (5)°) in **9**.

(III) Other Considerations. (a) s Character. In a qualitative valence-bond description, bond lengths and angles are highly dependent on *hybridization* of the atom under consideration which in turn depends upon the electronegativity of the substituents attached to it. For atoms that satisfy the octet rule, it is observed that the bond angle increases while bond length(s) decreases as the s character of the hybrid orbital(s)

Table VII. Comparison of Geometrical Parameters for the $Y_4M_4X_4$ Core of Some Electronically Equivalent Cubane-like $(R_3Y)_4M_4X_4$ Clusters (R = C_6H_5, C_2H_5; Y = P, As; M = Cu, Ag; X = Cl, Br, I)

	$(Ph_3P)_4$-Ag_4Cl_4 (1)	$(Ph_3P)_4$-Ag_4Br_4 (2)	$(Ph_3P)_4$-Ag_4I_4 (3)	$(Et_3P)_4$-Ag_4I_4 (4)	$(Ph_3P)_4$-Cu_4Cl_4 (5)	$(Et_3P)_4$-Cu_4Cl_4 (6)	$(Et_3P)_4$-Cu_4Br_4 (7)	$(Et_3P)_4$-Cu_4I_4 (8)	$(Et_3As)_4$-Cu_4I_4 (9)
Ref	*a*	*b*	*c*	*d*	*e*	*f*	*f*	*g*	*g*
Site symmetry	C_2-2	C_3-3	C_1-1	D_{2d}-$\bar{4}2m$	C_2-2	T_d-$\bar{4}3m$	T_d-$\bar{4}3m$	T_d-$\bar{4}3m$	T_d-$\bar{4}3m$
Space group	*Pbcn*	*R*3*c*	$P2_1/c$	$P4_2/nmc$	*Pbcn*	$I\bar{4}3m$	$I\bar{4}3m$	$I\bar{4}3m$	$I\bar{4}3m$
M···M av	3.633[i]	3.825	3.483	3.208	3.306	3.211 (2)	3.184 (2)	2.927 (2)	2.783 (2)
M···M min	3.408 (1)	3.719 (2)	3.115 (2)	3.198 (1)	3.118 (1)				
M···M max	3.797 (1)	3.930 (1)	3.768 (2)	3.229 (1)	3.430 (2)				
X···X av	3.837	4.082	4.582	4.753	3.576	3.657 (2)	3.932 (1)	4.380 (1)	4.424 (2)
X···X min	3.649 (5)	3.964 (2)	4.399 (2)	4.723 (1)	3.393 (3)				
X···X max	4.031 (3)	4.200 (1)	4.801 (2)	4.768 (1)	3.722 (3)				
M–X av	2.653	2.800	2.910	2.919	2.444	2.438 (1)	2.544 (1)	2.684 (1)	2.677 (2)
M–X min	2.532 (3)	2.677 (1)	2.836 (2)	2.918 (1)	2.363 (2)				
M–X max	2.760 (3)	2.962 (1)	3.037 (2)	2.919 (1)	2.505 (2)				
M–Y av	2.382	2.422	2.458	2.438 (2)	2.193	2.176 (2)	2.199 (2)	2.254 (3)	2.361 (2)
M–Y min	2.376 (3)	2.415 (5)	2.455 (4)		2.192 (2)				
M–Y max	2.388 (3)	2.429 (2)	2.462 (5)		2.193 (2)				
M–X–M av	86.48[j]	86.21	73.55	66.68	85.16 (6)	82.36 (5)	77.48 (4)	66.10 (4)	62.63 (5)
M–X–M min	79.32 (7)	82.35 (3)	64.53 (4)	66.44 (2)					
M–X–M max	92.67 (8)	92.39 (5)	81.07 (5)	67.15 (2)					
X–M–X av	92.72	93.67	104.08	109.01	94.12 (6)	97.15 (4)	101.25 (3)	109.38 (4)	111.45 (5)
X–M–X min	87.23 (8)	89.19 (3)	95.16 (5)	108.00 (2)					
X–M–X max	101.20 (8)	100.29 (4)	115.38 (5)	109.52 (2)					
Y–M–X av	122.35	122.32	114.11	109.93	122.02 (8)	120.02 (3)	116.80 (2)	109.56 (8)	107.41 (6)
Y–M–X min	109.88 (9)	106.94 (6)	104.07 (11)	109.13 (6)					
Y–M–X max	138.85 (9)	142.36 (6)	123.53 (12)	110.33 (3)					
Y···O[h]	4.607	4.764	4.591	4.402	4.218	4.142	4.149	4.046	4.065

[a] This work. [b] Reference 39. [c] Reference 40. [d] Reference 41. [e] Reference 32. [f] Reference 31. [g] Reference 30. [h] Calculated distance (Å) between the pnicogen atom Y and the centroid of the cubane-like core based upon the average M···M and M–Y distances assuming an idealized T_d geometry: $Y\cdots O = ({}^3/_8)^{1/2}(M\cdots M) + (M\text{–}Y)$. [i] All distances in angstroms. [j] All angles in degrees.

utilized by the central atom increases. It is also believed that atomic s character tends to concentrate in orbitals that are directed toward electropositive substituents or, equivalently, atomic p character tends to concentrate in orbitals that are directed toward electronegative groups. Since unshared electron pairs can be conceptually regarded as electrons in an orbital directed toward a void of zero electronegativity, a corollary of this theorem is that atoms tend to concentrate its s character in orbital(s) occupied by unshared electron pair(s) as the electronegativity of the substituents increases or as the electronegativity of the atom itself decreases.[57] While these simple ideas gain wide acceptance for main-group elements (where the valence shell is composed of only four orbitals, namely, one s and three p), they find little use in transition metal chemistry because of the incomplete valence d shell. However, for transition metal atoms with a spherically symmetric d shell such as d^0, d^5 (high spin), and d^{10} systems, these simplified valence-bond treatments can be invoked, at least qualitatively, to correlate trends of bond distances and interbond angles among a closely related series of molecules.[58]

We shall proceed by examining the bond lengths and angles at each metal and halogen site, assuming an idealized T_d geometry for the cubane-like molecule.

First, consider a metal atom (M) bonded to three bridging halogens (X) and one terminal ligand atom (Y) in a C_{3v} arrangement (YMX_3). Each metal atom can be considered, neglecting the filled d shell, as approximately, "sp^3" hybridized. As the electronegativity of the bridging halogen atom decreases along the sequence Cl > Br > I, the metal atom uses more s character in M–X bonding and, consequently, less s character (or more p character) in M–Y bonding. These trends lead to the prediction that, other things being equal, the X–M–X angles should increase (equivalently, Y–M–X should decrease) whereas the M–Y bond length should lengthen. This is exactly which is observed in the two series $(Ph_3P)_4Ag_4X_4$ and $(Et_3P)_4Cu_4X_4$ (cf. Table VII). For example, the average X–Ag–X angle increases from 92.72 to 93.67 to 104.08° (average P–Ag–X angle decreases from 122.35 to 122.32 to 114.11°) while the average Ag–P bond length increases from 2.382 to 2.422 to 2.458 Å for X = Cl (**1**), Br (**2**), and I (**3**) in $(Ph_3P)_4Ag_4X_4$, respectively. Similar trends are observed in $(Et_3P)_4Cu_4X_4$: the average X–Cu–X angle varies from 97.15 (4) to 101.25 (3) to 109.38 (4)°, the average P–Cu–X angle, from 120.02 (3) to 116.80 (2) to 109.56 (8)°, and the average Cu–P bond length from 2.176 (2) to 2.199 (2) to 2.254 (3) Å, for X = Cl, Br, and I, respectively.

Second, consider a triply bridging halogen atom (X) surrounded by three metal atoms (M) and a lone electron pair in a C_{3v} array ($:MX_3$). As the electronegativity of the halogen X decreases, it tends to concentrate its s character in the unshared electron pair, thereby leaving more p character for the M–X bonding which results in smaller M–X–M angles. This is also in accord with the experimental evidence (cf. Table VII).

(b) Nonbonded Attractions.[59] The possibility of indirect residual metal···metal bonding interactions via the triply bridging halogens, however, cannot be ruled out completely. Assuming that the p orbitals of the bridging halogen atom (X) lie lower in energy than the a_1 and e combinations of the "hybrid" orbitals utilized by the three metal atoms (M) for M–X bonding, the donation of electron densities from p_z of X to the symmetrical a_1 combination of the M_3 moieties will be larger than the donation of electron densities from (p_x, p_y) of X to the antisymmetrical e combinations simply because the energetic difference between the former pair of orbital combinations is smaller than that in the latter.[60] This in essence produces some *indirect* residual M···M bonding effect, thereby reducing the nonbonded M···M repulsions due to *direct* metal···metal interaction. As the electronegativity of X decreases (or equivalently as the electronegativity of M increases), the donation of electron density from X to M_3 is increased (because the p level of X is raised and becomes closer in energy to the M_3 levels) and the residual M···M bonding is enhanced. This causes the metal atoms to move closer together to take advantage of the location of larger electron density, resulting in smaller M···M distances and smaller M–X–M angles. This prediction is borne out in the following observations: (1) in $(Ph_3P)_4Ag_4X_4$, average Ag–X–Ag decreases from 86.48° (X = Cl) to 86.21° (X = Br) to 73.55° (X = I) accompanied by a change of average Ag···Ag distance from 3.633 to 3.825 to 3.483 Å; (2) in $(Et_3P)_4Cu_4X_4$, Cu–X–Cu decreases from 82.36 to 77.48 to 66.10° whereas Cu···Cu decreases from 3.211 to 3.184 to 2.927 Å for X = Cl, Br, and I, respectively. However, it must be emphasized that the overall M···M interactions are still repulsive because the direct contributions outweigh the indirect ones.

In conclusion, the interesting stereochemical variation of the $(R_3Y)_4M_4X_4$ family can be accomodated by a number of existing valency models. These models are by no means exclusive; they merely represent or emphasize certain aspects of various factors dictating the molecular geometry of these cluster systems.

Registry No. **1**, 54937-08-5; **2**, 59753-07-0; **3**, 54937-07-4; **4**, 55853-47-9; **5**, 50409-58-0; **6**, 55606-52-5; **7**, 55606-53-6; **8**, 51364-98-8; **9**, 51364-97-7.

Supplementary Material Available: Table of observed and calculated structure factors (12 pages). Ordering information is given on any current masthead page.

References and Notes

(1) (a) Bell Laboratories. (b) University of Wisconsin.
(2) M. A. Neuman, Trinh-Toan, and L. F. Dahl, *J. Am. Chem. Soc.*, **94**, 3383 (1972).
(3) Trinh-Toan, W. P. Fehlhammer, and L. F. Dahl, *J. Am. Chem. Soc.*, **94**, 3389 (1972).
(4) (a) C. H. Wei, G. R. Wilkes, P. M. Treichel, and L. F. Dahl, *Inorg. Chem.*, **5**, 900 (1965); (b) R. A. Schunn, C. J. Fritchie, Jr., and C. T. Prewitt, *ibid.*, **5**, 892 (1966).
(5) Trinh-Toan, W. P. Fehlhammer, and L. F. Dahl, to be submitted for publication.
(6) Trinh-Toan, B. K. Teo, W. P. Fehlhammer, and L. F. Dahl, to be submitted for publication.
(7) G. L. Simon and L. F. Dahl, *J. Am. Chem. Soc.*, **95**, 2175 (1973).
(8) G. L. Simon and L. F. Dahl, *J. Am. Chem. Soc.*, **95**, 2164 (1973).
(9) R. S. Gall, C. T.-W. Chu, and L. F. Dahl, *J. Am. Chem. Soc.*, **96**, 4017 (1974).
(10) R. S. Gall, N. G. Connelly, and L. F. Dahl, *J. Am. Chem. Soc.*, **96**, 4019 (1974).
(11) (a) B. K. Teo, Ph.D. Thesis, University of Wisconsin, 1973; (b) B. K. Teo and L. F. Dahl, to be submitted for publication.
(12) (a) B. A. Averill, T. Herskovitz, R. H. Holm, and J. A. Ibers, *J. Am. Chem. Soc.*, **95**, 3523 (1973).
(13) L. Que, Jr., M. A. Bobrik, J. A. Ibers, and R. H. Holm, *J. Am. Chem. Soc.*, **96**, 4168 (1974).
(14) C. Y. Yang, K. H. Johnson, R. H. Holm, and J. G. Norman, Jr., *J. Am. Chem. Soc.*, **97**, 6596 (1975).
(15) J. A. Bertrand, A. P. Ginsberg, R. I. Kaplan, C. E. Kirkwood, R. L. Martin, and R. C. Sherwood, *Inorg. Chem.*, **10**, 240 (1971).
(16) V. Albano, P. Bellon, G. Ciani, and M. Manassero, *Chem. Commun.*, 1242 (1969).
(17) U. Sartorelli, L. Garlaschelli, G. Ciani, and G. Bonora, *Inorg. Chim. Acta*, **5**, 191 (1971).
(18) A. S. Foust and L. F. Dahl, *J. Am. Chem. Soc.*, **92**, 7337 (1970).
(19) D. Bright, *Chem. Commun.*, 1169 (1970).
(20) W. Harrison, W. D. Marsh, and J. Trotter, *J. Chem. Soc., Dalton Trans.*, 1009 (1972).
(21) R. N. Margreaves and M. R. Trutter, *J. Chem. Soc. A*, 390 (1971).
(22) R. E. Rundle and J. H. Sturdivant, *J. Am. Chem. Soc.*, **69**, 1561 (1947).
(23) G. Donnay, L. B. Coleman, N. G. Krieghoff, and D. O. Cowan, *Acta Crystallogr., Sect. B*, **24**, 157 (1968).
(24) (a) H. S. Preston, J. C. Mills, and C. H. L. Kennard, *J. Organomet. Chem.*, **14**, 447 (1968); (b) T. G. Spiro, D. H. Templeton, and A. Zalkin, *Inorg. Chem.*, **7**, 2165 (1968).
(25) H. M. M. Shearer and C. B. Spencer, *Chem. Commun.*, 194 (1966).
(26) F. Schindler, H. Schmidbauer, and U. Kruger, *Angew. Chem., Int. Ed. Engl.*, **4**, 876 (1965).
(27) G. Dittmar and E. Hellner, *Angew. Chem., Int. Ed. Engl.*, **8**, 679 (1969).
(28) A. F. Wells, *Z. Kristallogr., Kristallgeom., Kristallphys., Kristallchem.*, **94**, 447 (1936).

(29) F. G. Mann, D. Purdie, and A. F. Wells, *J. Chem. Soc.*, 1503 (1936).
(30) M. R. Churchill and K. L. Kalra, *Inorg. Chem.*, **13**, 1899 (1974).
(31) M. R. Churchill, B. G. DeBoer, and S. J. Mendak, *Inorg. Chem.*, **14**, 2041 (1975).
(32) M. R. Churchill and K. L. Kalra, *Inorg. Chem.*, **13**, 1065 (1974).
(33) M. R. Churchill and K. L. Kalra, *Inorg. Chem.*, **13**, 1427 (1974).
(34) M. R. Churchill, B. G. DeBoer, and D. J. Donovan, *Inorg. Chem.*, **14**, 617 (1975).
(35) W. R. Clayton and S. G. Shore, *Cryst. Struct. Commun.*, **2**, 605 (1973).
(36) (a) N. Marsich, G. Nardin, and L. Randaccio, *J. Am. Chem. Soc.*, **95**, 4053 (1973); (b) G. Nardin and L. Randaccio, *Acta Crystallogr., Sect. B*, **30**, 1377 (1974); (c) A. Camus, G. Nardin, and L. Randaccio, *Inorg. Chim. Acta*, **12**, 23 (1975).
(37) F. G. Mann, A. F. Wells, and D. Purdie, *J. Chem. Soc.*, 1828 (1937).
(38) B. K. Teo and J. C. Calabrese, *J. Am. Chem. Soc.*, **97**, 1256 (1975).
(39) B. K. Teo and J. C. Calabrese, *J. Chem. Soc., Chem. Commun.*, 185 (1976).
(40) B. K. Teo and J. C. Calabrese, *Inorg. Chem.*, following paper in this issue.
(41) M. R. Churchill and B. G. Deboer, *Inorg. Chem.*, **14**, 2502 (1975).
(42) "International Tables for X-Ray Crystallography", Vol. I, 2d ed, Kynoch Press, Birmingham, England, 1965, p 149.
(43) R. A. Sparks et al., "Operations Manual. Syntex P$\bar{1}$ Diffractometer", Syntex Analytical Instruments, Cupertino, Calif., 1970.
(44) The absorption correction program DEAR (J. F. Blount) uses the Gaussian integration method of W. R. Busing and H. A. Levy, *Acta Crystallogr.*, **10**, 180 (1957).
(45) The integrated intensity (I) was calculated according to the expression $I = [S - (B_1 + B_2)/B_R]T_R$ where S is the scan counts, B_1 and B_2 are the background counts, B_R is the ratio of background time to scan time, and T_R is the 2θ scan rate in degrees per minute. The standard deviation of I was calculated as $\sigma(I) = T_R[S + (B_1 + B_2)/B_R^2 + (pI)^2]^{1/2}$.
(46) All least-squares refinements were based on the minimization of $\sum w_i||F_o| - |F_c||^2$ with the individual weights $w_i = 1/\sigma(F_o)^2$. Atomic scattering factors used for all nonhydrogen atoms are from H. P. Hanson, F. Herman, J. D. Lea, and S. Skillman, *Acta Crystallogr.*, **17**, 1040 (1964); those for the hydrogen atoms are from R. F. Stewart, E. R. Davidson, and W. T. Simpson, *J. Chem. Phys.*, **42**, 3175 (1965).
(47) Hydrogen atoms were calculated at C–H distances of 1.00 Å and assigned constant isotropic thermal parameters of 7.00 Å^2.
(48) $R_1 = [\sum||F_o| - |F_c||/\sum|F_o|] \times 100\%$ and $R_2 = [\sum w_i||F_o| - |F_c||^2/\sum w_i|F_o|^2]^{1/2} \times 100\%$. See supplementary material for a listing of observed and calculated structure factors.
(49) "International Tables for X-Ray Crystallography", Vol. III, Kynoch Press, Birmingham, England, 1962, p 215.
(50) C. K. Johnson, *J. Appl. Crystallogr.*, **6**, 318 (1973): ORTEP2.
(51) *Chem. Soc., Spec. Publ.*, **No. 18**, S3s (1965).
(52) K. Aurivillius, A. Cassel, and L. Falth, *Chem. Scr.*, **5**, 9 (1974).
(53) van der Waals radii of Cl (1.80 Å), Br (1.95 Å), I (2.15 Å), and H (1.20 Å) are taken from L Pauling, "The Nature of the Chemical Bond", 3d ed, Cornell University Press, Ithaca, N.Y., 1960, p 260.
(54) The following estimated single-bond covalent radii were taken from L. Pauling, "The Nature of the Chemical Bond", 3d ed, Cornell University Press, Ithaca, N.Y., 1960, pp 224, 256: Cl, 0.99 Å; Br, 1.14 Å; I, 1.33 Å; P, 1.10 Å; As, 1.21 Å; Cu, 1.17 Å; Ag, 1.34 Å.
(55) L. F. Dahl, E. Rodulfo de Gil, and R. D. Feltham, *J. Am. Chem. Soc.*, **91**, 1653 (1969).
(56) Using space-filling Courtauld atomic models from Griffin and Georgy Ltd., Wembley, Middlesex, England, the van der Waals volumes of an ethyl and of a phenyl group are measured to be approximately 35 and 83 Å^3, respectively.
(57) H. A. Bent, *J. Chem. Educ.*, **37**, 616 (1960).
(58) Based on an extensive ^{31}P NMR studies, the s character of Ag–P bonds for various hybridizations has been discussed by E. L. Muetterties and C. W. Alegranti, *J. Am. Chem. Soc.*, **94**, 6386 (1972).
(59) P. Kollman, *J. Am. Chem. Soc.*, **96**, 4363 (1974).
(60) B. K. Teo, M. B. Hall, R. F. Fenske, and L. F. Dahl, *Inorg. Chem.*, **14**, 3103 (1975).

Contribution from Bell Laboratories, Murray Hill, New Jersey 07974, and the Department of Chemistry, University of Wisconsin, Madison Wisconsin 53706

Stereochemical Systematics of Metal Clusters. Crystallographic Evidence for a New Cubane ⇌ Chair Isomerism in Tetrameric Triphenylphosphine Silver Iodide, $(Ph_3P)_4Ag_4I_4$

BOON-KENG TEO*[1a] and JOSEPH C. CALABRESE[1b]

Received March 26, 1976 AIC602339

The tetrameric triphenylphosphine silver iodide, obtained by the reaction of triphenylphosphine with silver iodide, has been shown by single-crystal x-ray diffraction studies to exist in either a cubane- or a chair-like structure in the solid state. Slow crystallization of this complex from chloroform/ether afforded monoclinic crystals of centrosymmetric space group $P2_1/c$ with $a = 24.991$ (5) Å, $b = 12.402$ (3) Å, $c = 25.074$ (6) Å, $\beta = 113.30$ (7)°, $V = 7137$ (3) Å^3, and $Z = 4$. A complete structural analysis, with final reliability indices of $R_1 = 4.83\%$ and $R_2 = 5.63\%$, revealed a cubane-like configuration defined by two interpenetrating silver and iodine tetrahedra situated on alternate corners of a highly distorted cube, with each silver atom being further coordinated to a triphenylphosphine ligand. The unusual degree of distortion from the idealized T_d molecular symmetry is manifest in that the silver···silver distances span from 3.115 (2) to 3.768 (2) Å (3.483 Å (average)), the iodine···iodine distances vary from 4.399 (2) to 4.801 (2) Å (4.582 Å (average)), and the silver–iodine bond lengths range from 2.836 (2) to 3.037 (2) Å (2.910 Å (average)). On the other hand, slow crystallization of $(Ph_3P)_4Ag_4I_4$ from methylene chloride/ether produced triclinic crystals of centrosymmetric space group $P\bar{1}$ with $a = 12.102$ (3) Å, $b = 15.071$ (2) Å, $c = 11.948$ (2) Å, $\alpha = 110.59$ (1)°, $\beta = 96.40$ (2)°, $\gamma = 71.64$ (2)°, $V = 1936$ (1) Å^3, and $Z = 1$ ($(Ph_3P)_4Ag_4I_4 \cdot 1.5CH_2Cl_2$). Structural analysis yielded $R_1 = 4.50\%$ and $R_2 = 6.52\%$. The molecule has a crystallographically imposed C_i-$\bar{1}$ symmetry with the Ag_4I_4 core defining a chair-like configuration. The silver···silver, iodine···iodine, and silver–iodine distances range from 3.095 (1) to 4.315 (2), 4.505 (1) to 4.763 (1), and 2.724 (1) to 2.995 (1) Å, respectively. The silver–iodine bond lengths can be correlated with the coordination numbers of the silver and/or the iodine atoms. This unprecedented type of isomerism allows a direct stereochemical comparison between the cubane and the chair configurations. The intriguing stereochemical variations of the $(R_3Y)_4M_4X_4$ (R = C_6H_5, C_2H_5; Y = P, As; M = Cu, Ag; X = Cl, Br, I) family are rationalized in terms of intramolecular van der Waals repulsions involving the bulkyl terminal ligands and the bridging halogens.

Introduction

As part of a continuing effort to elucidate *electronic*[2-9] *vs. steric*[10-14] effects in dictating the stereochemistries of tetrameric metal cluster systems possessing a M_4X_4 (M = metal; X = bridging ligand) core, we wish to report the synthesis and structural characterization of the title compound.[11a] Rather unexpectedly, we have found that $(Ph_3P)_4Ag_4I_4$ is capable of existing in both a highly distorted cubane-like configuration (I) and a chair-like structure (II) in solid state.

This unprecedented type of isomerism provides an excellent opportunity for a *direct* comparison of accurate molecular parameters of both forms which, along with other analogous